January 2017

Patterns of Total Gaseous Mercury Variation Prior to and After Brownfield Remediation in Syracuse, NY

Linghui Meng
Syracuse University

Abstract

Although mercury toxicity has been recognized for centuries, the atmospheric cycle of this element is still not fully understood. In order to obtain a better perspective of the dynamics of atmospheric mercury in urban areas, total gaseous mercury (TGM) was measured at a brownfield site at the Center of Excellence (CoE) in Syracuse NY from 2011 to 2016. The brownfield was removed on May 2015, and a parking lot was installed. For this study, I had a series of objectives including: (1) to understand vertical and temporal variations in TGM concentration; (2) investigate the influence of meteorological factors on TGM concentrations and variations; (3) evaluate the effect of brownfield removal and site restoration on TGM concentrations and variations; (4) compare TGM variation at this site with other monitoring sites in New York State to confirm hypothesis made in this study. Continuous TGM measurements were made at two different heights (1.8 m and 42.7 m) at the COE. To interpret TGM variations, meteorological data collected by SUNY-ESF were also used in this analysis. In addition, mercury flux measurements from the land surface was conducted at this site on June 2015. Prior to brownfield remediation, the overall average TGM concentrations were 1.6±0.58 ng/m^3 and 1.4±0.40 ng/m^3 at ground and upper level, respectively. TGM tended to have higher concentrations during night and in the morning, and was positively correlated with air temperature, solar radiation, but negatively correlated with wind speed. After brownfield remediation, TGM concentrations immediately decreased by 32% and 22% at the ground and upper level, respectively and likely to have higher concentrations during nighttime and lower

concentrations in the daylight. Relations of TGM concentrations with temperature, solar radiation and wind speed were completely eliminated after brownfield remediation. These results suggest that TGM concentrations at this site were strongly controlled by local mercury evasion prior to brownfield removal, with evasion rate increasing due to higher air temperature and stronger solar radiation. TGM derived from mercury evasion from the site were diluted by horizontal mixing from winds and vertical mixing associated with movement of the PBL.

Patterns of Total Gaseous Mercury Variation Prior to and After Brownfield Remediation in Syracuse, NY

By

Linghui Meng

B.S., Minzu University of China, 2012

Thesis

Submitted in partial fulfillment of the requirements for the degree of

Master of Science in Environmental Engineering Science

Syracuse University

May 2017

Acknowledgements

This study is guided by Dr. Charles Driscoll. I would like to express my heartfelt thanks to him for supporting me to finish my master's thesis. I'd like to thank Mario Montesdeoca, Paul K. McCathy and Patrick McHale for their support and association during this project. I also thank Drs. David Gay and Huiting Mao for providing mercury data collected at AMN sites and SUNY-ESF campus, and Dr. Myron Mitchell and Geoffrey Millard for providing meteorological data. I would like to thank US EPA, NOAA and Syracuse Hancock International Airport for data provided for this study.

Table of Contents

List of Illustrative materials

1.1 Use and Effects of Mercury

Mercury is a naturally occurring metallic element. Before mercury bio-toxicity was widely recognized, it was widely used for medical applications, measuring devices, paint, as a fungicide and other applications. Aside from being used in fluorescent lamps, most mercury products have been gradually replaced by less toxic alternatives due to health concerns (Surmann and Zeyat, 2005).

Several forms of mercury exist, including elemental mercury, oxidized mercury, and methyl mercury. Studies have shown that mercury toxicity varies with the mercury forms and dose (Bernhoft, 2012). Elemental mercury damages the brain and nervous system. Chronic exposure to low levels of elemental mercury causes weakness, fatigue, anorexia and weight loss and will induce severe pneumonitis and cause death in extreme cases (Bernhoft, 2011). Oxidized mercury impacts the intestine and kidney function. Methyl mercury strongly bioaccumulates and is a neurotoxin. Mercury pollution can seriously affect public health. Minamata, first reported in Japan in 1956, is the most well-known disease caused by methyl mercury. Its symptoms include ataxia, muscle weakness, and impaired in hearing and speech. In extreme cases, it causes insanity, paralysis, coma, and death within a few weeks after the onset of symptoms. There are 2265 victims of Minamata that have been officially recognized by the Japanese government, 1784 of these have died. Mercury is released to the environment from fossil fuel combustion, industrial activities, mining and other human activities resulting in concern about the potential health risk associated with the formation of toxic methylmercury (Amos et al., 2013)

1.2 Mercury in the Environment

1.2.1 Mercury in the Environment

There is a dynamic cycle of mercury in the environment. Most of mercury exists as stable compounds and stores in the Earth's crust. The average concentration of mercury in the Earth's crust is 0.08 μg/g (Ehrlich and Newman, 2008). Mercury is released naturally by volcanic eruptions, and oxidation and weathering processes of rocks and minerals. Much of the mercury released by human or natural processes cycles through the atmosphere (Driscoll et al., 2013). The ultimate fate of this mercury is soil or ocean sediments. A small proportion of the released mercury is dissolved, transported and processed in water. Mercury cycles through various biological process including plant uptake, release to detrital pool and the atmosphere, and accumulates along food chains. According to Driscoll et al (2013), 1000 Gg mercury is in soil, 357 Gg mercury is dissolved in ocean water, and 5 Gg Mercury is in the atmosphere, but there is no reliable estimate of the mercury pool in the biosphere.

1.2.2 Atmospheric Cycle of Mercury

1.2.2.1 Mercury Species in Atmosphere

There are three forms of mercury in air: gaseous elemental mercury (GEM), reactive gaseous mercury (RGM), and particulate-bound mercury (PBM). GEM has stable physical and chemical properties, and its lifetime has been reported to range from 0.5 to 2 years (Parsons et al., 2013). RGM is an oxidation product of GEM but can also be directly emitted from human sources, and has a lifetime ranging from

hours to days in the atmosphere. PBM is a product of RGM absorbed by particulates, it is largely found in the fine fraction (≤2.5μm), but can also occur in the coarse fraction of particulate matter (>2.5μm) (Keeler et al., 1995). The lifetime of PBM depends on particle diameter, and is generally less than 10 days (Schroeder & Munthe, 1998). In this study, we measured the concentration of total gaseous mercury (TGM), which is a sum of GEM and RGM.

1.2.2.2 Mercury Sources

Atmospheric mercury emissions include natural and anthropogenic sources. Natural sources are biotic and abiotic natural processes that produce atmospheric mercury, which includes mercury emissions from terrestrial and aquatic surfaces, volcano eruptions, and biomass burning. According to Selin (2009), mercury emissions from water surfaces is the largest natural mercury source (5000 $Mg \cdot yr^{-1}$), followed by mercury emissions from land surfaces (1100 $Mg \cdot yr^{-1}$), biomass burning (600 $Mg \cdot yr^{-1}$) and volcano eruptions (500 $Mg \cdot yr^{-1}$). UNEP (2013) estimated that mercury emissions from water surfaces is 2000-2950 $Mg \cdot yr^{-1}$, followed by mercury emission from soil and vegetation surfaces (1700-2800 $Mg \cdot yr^{-1}$), biomass burning (300-600 $Mg \cdot yr^{-1}$) and volcano eruptions (80-600 $Mg \cdot yr^{-1}$).

Anthropogenic mercury sources include fossil fuel combustion, mining, smelting and production of metals, cement production, oil refining, emissions from contaminated sites, artisanal and small-scale gold mining, chlor-alkali industry, consumer products, waste incineration and others (Pirrone et al., 2010). There are a variety of estimates of the total amount of mercury released from anthropogenic

sources. Pirrone et al. (2000) estimated that annual human mercury discharge is 2239 $Mg \cdot yr^{-1}$, Selin (2009) estimated 3400 $Mg \cdot yr^{-1}$, and UNEP (2013) estimated 2000 $Mg \cdot yr^{-1}$.

Note that mercury is not only derived from direct emission but mercury deposited from atmosphere to the Earth's surface also can be reemitted to the atmosphere as a secondary emission sources. Grigal suggested that up to 80% of deposited mercury on land surface is remitted to the atmosphere (Grigal, 2002).

1.2.2.3 Mercury Transformation and Transport

Atmospheric mercury transformations include GEM oxidation and RGM reduction. GEM oxidation to RGM can be mediated by O_3, ·OH (Lin & Pehkonen, 1997), Br· (Holmes et al., 2010) and Cl· (Impey et al., 1997). Meanwhile RGM can be reduced by solar radiation in association with particulates. Kunkely et al. (1997) reported that several mercuric complexes decompose and release GEM associates with UV light. This reaction is thought to occur in the upper troposphere. There is no evidence to show it occurs in the lower troposphere. RGM reduction at lower troposphere occurs in the aqueous phase (Ericksen et al., 2005) and on snow surfaces (Dommergue et al., 2012), which are accelerated with light.

GEM has a long residence time in the atmosphere due to its stable properties (0.5-2 years), which allows for long distance or even continental scale transport (Petersen et al., 1995). Observations at the Harvard Forest shows clear evidence of long-distance transport of gaseous mercury in a smoke plume from forest fires in northern Quebec, Canada (Sigler et al., 2004). Several studies have suggested that

East Asia is an important regional anthropogenic mercury source, and is an important input to North American (Seigneur et al., 2004; Selin & Jacob, 2008; Weiss-Penzias et al., 2007).

1.2.2.4 Mercury Fate

Dry and wet deposition are two pathways by which atmospheric mercury reaches the Earth's surface. Dry deposition is gaseous and particulate mercury deposited to ground or water surfaces. All mercury species can be removed by dry deposition, with the greatest flux occurring as GEM. Mercury wet deposition is atmospheric mercury washed out by precipitation. The dominant mercury species removed by wet deposition are RGM and PBM due to their high water-solubility. Selin et al. (2009) estimated that deposition removed 4100 Mg mercury from the atmosphere to land and 7100 Mg mercury to the oceans. Note that the mercury lost through deposition may not be permanently removed from the atmospheric cycle. The mercury deposited to land surface can be re-emitted into the atmosphere by reduction followed by evasion.

1.3 Atmospheric Mercury Patterns

1.3.1 Distribution of Atmospheric Mercury

The distribution of mercury in the atmosphere is not homogenous. Background concentrations of GEM at sea level are 1.5-1.7 ng/m^3 in the Northern Hemisphere and 1.1-1.5 ng/m^3 in the Southern Hemisphere (Lindberg et al., 2007). Aircraft observations revealed the atmospheric mercury concentration is homogeneous in the troposphere, and sharply decreases in the lower stratosphere (Talbot et al. 2007). Whereas, mercury concentrations under boundary layer are not homogeneous. A study

of mercury in Toronto reported an increase in TGM concentrations with increasing sampling height (3.5, 7, 12 m) from the land surface (Denis et al. 2006; Song et al. 2009).

1.3.2 Trends in Atmospheric Mercury Concentrations

The mercury concentration in the atmosphere has not been constant over time. A study of an ice core collected at Wyoming suggests the mercury deposition has increased in recent centuries (Schuster, et al., 2002). This pattern is likely an indication of an increase in atmospheric mercury concentrations. Two sharp increases in mercury deposition were observed from the ice core. One increase occurred in the late 1800s, which corresponds with the gold rush in North American. The other increase occurred in the late 1900s, which corresponds with increase in coal-fired power plants (UNEP, 2013). However, direct observations have revealed a decrease in atmospheric mercury concentration in recent decades. Slemr et al. (2011) has reported a 20 to 38% decrease in GEM concentration since 1996 from continuous mercury measurements in North America. The current decreasing trend in mercury concentrations is thought to be a result of decrease in mercury emissions. Zhang et al., (2016) investigated global mercury emission inventories and reported a decrease in mercury emissions, with a 20% decrease of total mercury emissions and a 30% decrease in anthropogenic emissions at the global scale.

1.3.3 Mercury Seasonal Variation

There are several different seasonal patterns of GEM concentration have been reported in the literature. For example, GEM often has the highest concentration in

summer and the lowest concentration in winter (Kim et al., 2011; Xin Lan et al., 2014; Zhu et al., 2012). This pattern is believed to be the result of high soil mercury emissions in summer. Mercury has also been shown to have higher concentrations in summer and winter, but lower concentrations in spring and fall (Denis et al, 2006; Poissant et al., 2005). This pattern is attributed to increased emissions from anthropogenic sources associated with reduced GEM oxidation in winter and higher mercury emission and re-emissions from the land surface due to high air temperature in summer. There are also reports of sites having high GEM concentrations in winter. There are two possible explanations for this pattern. Stamenkovic et al. (2007) suggested that this pattern is due to temperature inversion and reduced photo-oxidation in winter, while Schroeder and Munthe (1998) explained this pattern by reduced boundary layer height coupled with enhanced anthropogenic emissions in winter.

1.3.4 Mercury Diurnal Variation

Three types of diurnal patterns of atmospheric mercury concentrations have been frequently reported in the literature. First, mercury concentrations decrease at night reaching a minimum before sunrise, and then gradually increase reaching a maximum before noon (Cchoi et al., 2013; Kellerhals et al., 2003; Lan et al., 2012; Mao et al., 2016). This pattern is thought to be caused by an increase in soil mercury evasion with increasing air temperature and solar radiation associated with strong downward mixing in the morning, and increasing GEM oxidation in the afternoon. Second, mercury accumulates in the planetary boundary layer (PBL) overnight reaching a

maximum before sunrise, and then rapidly decreases reaching the minimum in the afternoon, and increases again after sunset. (Choi et al., 2013; Lan et al., 2014; Song et al., 2009; Mao et al., 2016). This pattern is considered to be the result of variation in the PBL under a relatively constant mercury release rate. The PBL height decreases with decreasing air temperature at night, causing GEM to accumulate under the boundary layer and concentrations to increase. After sunrise, the PBL height increases with increasing air temperature during daylight, diluting GEM and decreasing concentrations. Third, mercury remains at a constant concentration during the day, except for a rapid increase after sunrise. The rapid increase is thought to due to mercury from higher altitudes brought to the surface after residual layer erodes after sunrise (Lan et al., 2014; Stamenkovic et al, 2007), while others believe this pattern due to reduction of oxidized mercury from land surfaces by solar radiation (Schroeder et al, 1998).

1.4 The Influence of Meteorological Factors on Atmospheric Mercury Concentrations

1.4.1 Temperature

Studies have revealed temperature influences atmospheric mercury concentrations by several mechanisms, including increasing mercury evasion rate with increasing temperature; increases in GEM photooxidation rate with increasing temperature, and indirectly by increasing GEM dilution associated with increases in the PBL height with increases in air temperature. Gabriel et al. (2006) showed that the emission rate of GEM from grass covered soil was constant at 2-3 $ng \cdot m^{-2} \cdot h^{-1}$ at 10-

20℃, but increased to 7-8 $ng \cdot m^{-2} \cdot h^{-1}$ at 20-30℃. Choi et al. (2013) observed a negative correlation between GEM and air temperature as well as a positive correlation between RGM and air temperature. These correlations suggest an increase in GEM oxidation with increasing air temperature. Lan et al. (2014) reported a strong correlation between TGM mixing ratio and PBL height.

1.4.2 Solar Radiation

Solar radiation is considered to be an important factor influencing atmospheric mercury concentrations. Solar radiation is thought to accelerate GEM oxidation, and induces deposited mercury to be reduced and re-emited causing increase in mercury evasion rate. Gustin et al. (2002) reported that mercury emission rate from soil enhanced by 1.5 to 116 times under light compared with dark conditions. Schroeder and Munthe (1998) found that solar radiation can promote the reduction of deposited RGM to GEM, resulting in emissions to the atmosphere. Poissant et al. (2004) reported that RGM concentration was related to solar radiation, and suggested that GEM oxidation rate is enhanced by increasing solar radiation. RGM reduction is also thought to be enhanced by solar radiation. Kunkely et al. (1997) reported RGM reduction was accelerated by UV light in the upper troposphere. Studies suggest that RGM reduction also occurs in the aqueous phase (Ericksen et al., 2005) and on snow surface (Dommergue et al., 2012) associates with light.

1.4.3 Moisture

Research has shown that moisture influences atmospheric mercury

concentrations. Precipitation is considered as the dominant process removing water-soluble mercury from the atmosphere. Whereas, an increase in soil moisture is thought to increase mercury emissions from soil. Johnson et al. (2003) reported that precipitation input to dry soil increases soil GEM evasion. RGM reduction is thought to occur in the aqueous phase (Ericksen et al., 2005). Choi et al. (2013) showed that the GEM concentrations were significantly higher under high humidity condition (relative humidity > 80%) than that under lower humidity conditions, while RGM concentrations showed the opposite pattern. Soil moisture is thought to increase mercury absorption in soil (Poissant & Casimir, 1998; Siegel et al, 1988). However, Fang (1981) suggested that ability of soil to absorb mercury increases with soil moisture but reaches a maximum and then decreases.

1.4.4 Wind

Wind facilitates long distance transport of GEM from sources to remote sources, but dilutes high local TGM concentrations. Mercury derived from sources outside of region can significantly increases local mercury concentrations. Sigler et al. (2004) observed elevated gaseous mercury concentrations associated with a smoke plume from a forest fire in Canada. Liu et al. (2010) reported that GEM originating from the urban area of Detroit is an important source for a rural site downwind from the urban area. Note that air low in mercury can decrease local gaseous mercury concentrations. Lan et al. (2014) found that wind supplied clean marine air to the inland area in Houston diluting local TGM concentrations.

1.5 Mercury Studies in Urban Areas

Improving understanding of atmospheric mercury dynamics in the urban environment is an important research endeavor. The atmospheric cycle of mercury in urban landscapes is different from that of rural environments in several respects. First, human activities, including industrial activities and fossil fuel combustion release large amounts of mercury directly into the atmosphere increasing mercury concentrations. Second, the heat island effect, which is the result of ground surface modification associated with urbanization, increasing temperature produces local secondary circulation and alters the transport of mercury to the upper atmosphere. Third, mercury soil evasion in urban areas is lower than rural areas due to an abundance of impervious land cover which limits evasion. Gabriel et al (2006) showed that the average mercury evasion rate from pavement surface in Tuscaloosa, Alabama is 0.02 ng m^{-2} h^{-1}, much lower than from bare soil (6.48 ng m^{-2} h^{-1}). Fourth, structures in urban areas disrupt air exchange. Weakened air exchange associated with the asymmetrical distribution of mercury sources causes mercury concentrations to vary significantly among areas of a given city. Carpi and Chen (2002) in a study of New York City and Kim et al. (2011) in a study in Seoul, Korea observed spatial variations of GEM concentrations within cities.

Diurnal variations of GEM in urban areas are different from those in rural areas. Mercury studies in urban areas frequently report a diurnal pattern of GEM that accumulates overnight reaching a maximum before sunrise, rapidly decreasing after sunrise and reaching a minimum at sunset (Choi et al., 2013; Kim et al., 2011; Xin

Lan et al., 2014; Song et al., 2009). In contrast, studies in rural areas often report an pattern that GEM concentrations increase in the morning associated with increasing air temperature and solar radiation, and then decrease until the next sunrise (Choi et al., 2013; Kellerhals et al., 2003; Lan et al., 2014).

Mercury studies in urban areas have been conducted in North American, Europe, and East Asian. However, these studies were conducted at different heights from the land surface, ranging from 1.5m to 81m. Mercury studies conducted in Toronto suggest that GEM concentrations may vary with height from the land surface (Denis et al., 2006; Song et al., 2009). A vertical variation in GEM concentration limits the ability to compare of urban mercury studies conducted at different heights.

1.6 Scope of This Research

Most previous research on gaseous mercury concentrations has been conducted in rural areas. Only a few studies have examined mercury concentrations and its variation in urban settings. Fewer still have examined mercury variations from a land surface with given sampling locations at different heights. From a review of the literature, I have the following research questions: Do TGM concentrations at ground surface and height from the land surface exhibit similar diurnal and seasonal variations? What physical factors affect temporal variation in TGM concentration? Can a local brownfield be a source of urban TGM concentrations? To address these questions, TGM concentrations were measured at two heights (1.8 m and 42.3 m) at a brownfield site in Syracuse, NY. To interpret TGM variation, mercury evasion flux

data and meteorological data were obtained and evaluated over diurnal and seasonal timescales. During the study, the brownfield adjacent to the TGM measurement site was removed and a large impervious area (parking lot) was installed. I investigated the response of TGM concentrations to this land cover modification. Finally, I compared TGM measurements observed at this site with TGM measurements obtained at rural and urban sites in New York State.

2. Methods

2.1 Site Description

This study was conducted at the Urban Ecological Observation Tower (N 43° 3' 0.05", W 76° 8' 25.62") in Syracuse, NY. Syracuse is the fourth most populous city of New York State (144,669; 2013 Census). The region has a humid continental climate. Annual average temperature is 9.4℃, annual rainfall is 977 mm, and annual snowfall is 3145 mm. The tower is located in the urban core of Syracuse, adjacent to two major highways (rtes 81 and 690; Figure 1). Commercial buildings are positioned to the south and residential houses to the north of the tower. The dominant immediate land cover is impervious land, comprising 68% of the total area of 1 km^2 around the tower (Buckley et al., 2014). There was large area of brownfield adjacent to the tower, and approximately 150,000 ton of contaminated soil was removed in May 2015 for site restoration and parking construction (4,950 m^2). Mercury concentrations in the soil removed from the site ranged from 0.05 to 0.23 mg/g (N=18).

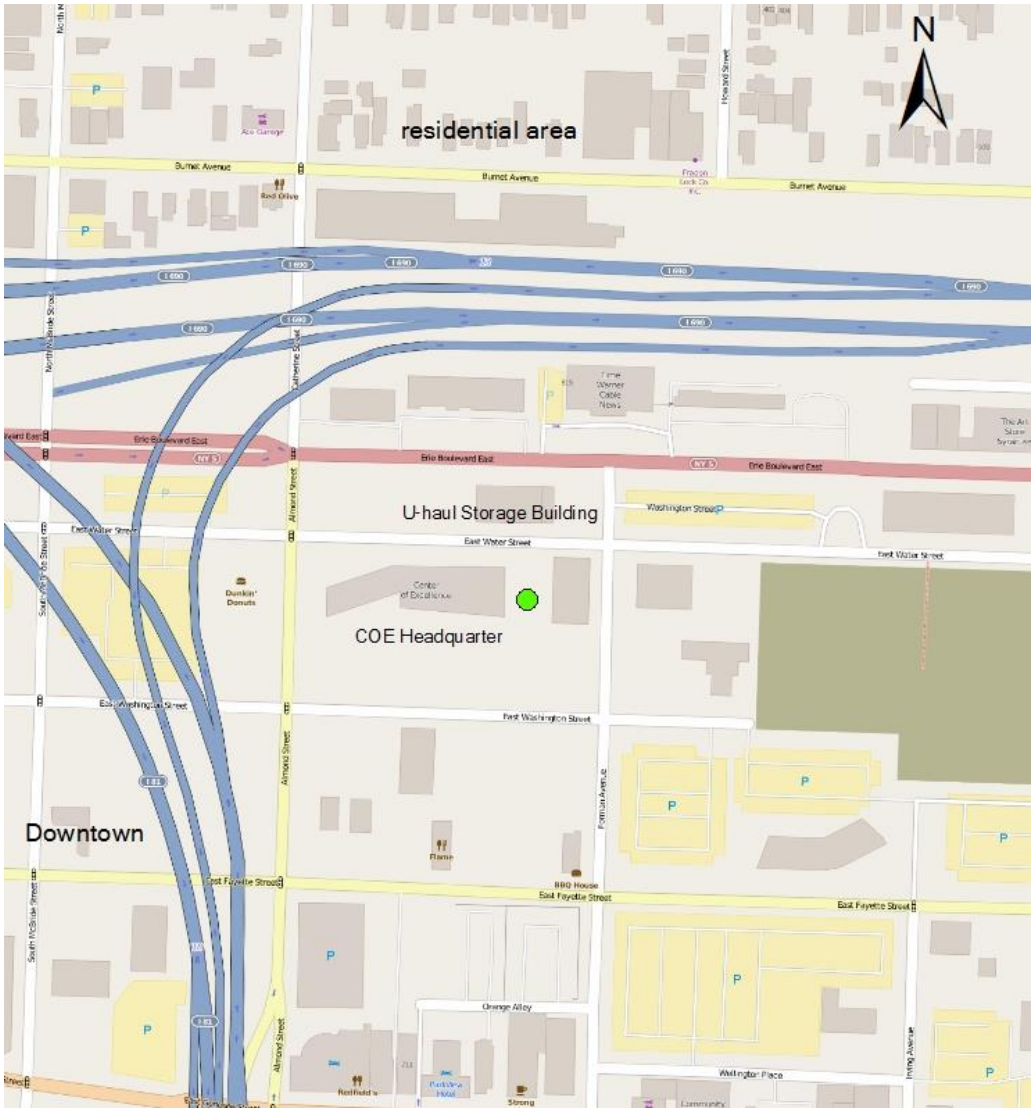

Figure 1. Sampling location of total gaseous mercury measurements in Syracuse, NY, USA.

2.2 Instrumentation

In this study, TGM concentration was measured using a Tekran 2537A mercury vapor analyzer to perform automatic, continuous long-term data collection. The 2537A analyzer uses cold vapor atomic fluorescence spectrometry (CVAFS) with a 0.1 ng/m^3 detection limitation. In the measurements, gaseous mercury in sampled air is initially captured by an internal gold matrix, and then it is released into an argon air flow and finally it is transported to a quartz cuvette. The gaseous mercury is then

illuminated by a low-pressure mercury vapor lamp and emits fluorescence which is quantified as voltage values by a photomultiplier tube. The gaseous mercury concentration shows a linear relationship with the voltage. To characterize the linear relationship for purpose of instruments calibration, the voltages of two mercury concentrations (0 and 27.1 ng/m^3) were measured. Zero mercury air (0 $\mathrm{ng} \cdot m^{-3}$) is produced by a zero mercury air generator and the sample of standard mercury (27.1 $\mathrm{ng} \cdot m^{-3}$) is produced by the permanent mercury source in the analyzer.

2.3 Sampling Methods

2.3.1 Atmospheric Mercury

In this study, the TGM in air was measured at two heights: ground (1.8 m) and upper (42.7 m) level (Figure 2). The sampling inlet at the ground level is adjacent to the observation tower and next to E. Water Street. The sampling inlet of upper level is located on the top of the observation tower. A pump was used to deliver air samples from the top of the tower to the mercury analyzer. TGM concentrations of sample air were measured twice at each inlet switched by a valve which controlled by the Model 1110 controller. A Model 1120 controller was also used to achieve a standard addition for quality control measurement. The TGM concentration was measured over three periods during the study (June 2011-July 2011, November 2011-June 2012, June 2015 to May 2016).

2.3.2 Mercury Evasion Flux Measurement

Soil mercury evasion was measured using a dynamic flux chamber during June 2015 after brownfield restoration (Figure 3). The dynamic flux chamber is a 3.87 L

clear polycarbonate vessel, with an 18.4cm diameter, which was sealed to the ground surface. To facilitate the air exchange rate in the chamber, 8 holes equally distanced 5 cm above the ground surface are positioned on the chamber wall. A Tekran 2537A mercury vapor analyzer was used to make separate measurements of TGM concentrations inside the dynamic flux chamber and of outside ambient air. One inlet connected to the top of the chamber was used to sample air inside the chamber. The other inlet was positioned next to the chamber, 5 cm above the ground surface. Duplicate measurements were taken at each inlet and switched via a valve unit controlled by a Model 1110 controller. Soil mercury evasion flux is calculated with equation 1:

$$F = (C_{chamber} - C_{ambient}) \times \frac{Q}{A} \quad [1]$$

F is mercury flux rate ($ng \cdot m^{-2} \cdot h^{-1}$);

$C_{chamber}$ is the TGM concentration of air inside the flux chamber ($ng \cdot m^{-3}$);

$C_{ambient}$ is the TGM concentrations of ambient air ($ng \cdot m^{-3}$);

Q is flow rate of flushing air ($L \cdot min^{-1}$); and

A is the area of soil exposed in the chamber (m^2).

In this study, Q is 4.4 $L \cdot min^{-1}$, A is 0.11 m^2.

Two pumps were used to circulate air inside the chamber. The GASF pump (3.4 $L \cdot min^{-1}$) was used to measure TGM concentrations of air inside the chamber and the KNF pump (5.9 $L \cdot min^{-1}$) was used to measure TGM concentrations of ambient air.

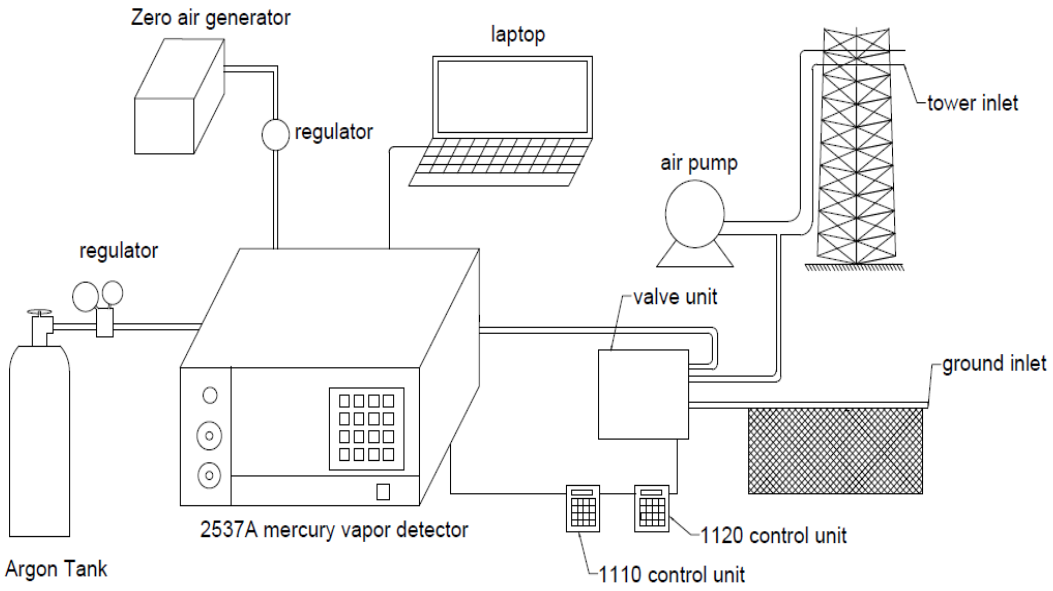

Figure 2. Schematic diagram of atmospheric TGM measurement system used in this study.

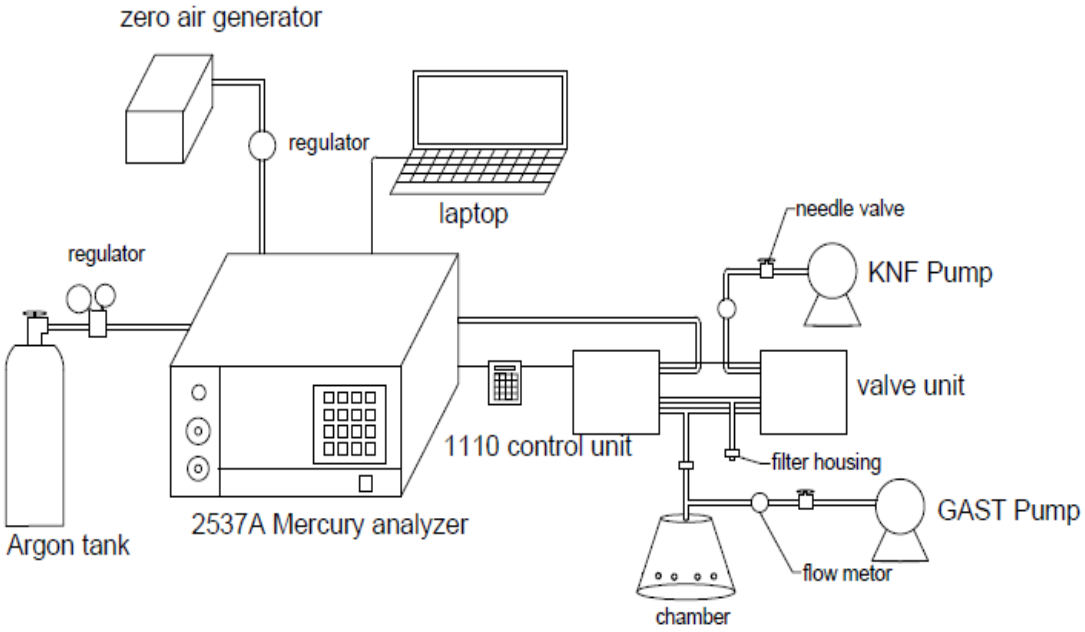

Figure 3. Schematic diagram of soil evasion measurement system used in this study.

2.4 Quality Assurance/ Quality Control

2.4.1 Automatic Calibration

The Tekran 2537A mercury vapor analyzer can achieve automatic calibration at set intervals. In this study, the calibration interval was 25 hours.

2.4.2 Standard Addition

The performance of the Tekran 2537A mercury analyzer was verified with standard addition from a permanent source inside the analyzer. The recovery rate of the standard addition is used to determine the performance of the analyzer. The analyzer is regarded as working effectively if recovery rate falls within the range of 80~120% of the standard. In this study, the standard addition occurred after every 35 measurements and the recovery rate was calculated with equation 2.

$$R = \frac{C_{measured} - C_{background}}{C_{theory}} \times 100\% \quad [2]$$

$C_{measured}$ is the actual mercury concentration detected by the 2537A analyzer ($ng \cdot m^{-3}$);

$C_{background}$ is the mercury concentration in ambient air ($ng \cdot m^{-3}$); and

C_{theory} is the theoretical mercury concentration ($ng \cdot m^{-3}$).

In this study, C_{theory} is 27.2 $ng \cdot m^{-3}$.

2.4.3 Manual Injection

The manual injection was used to examine the accuracy of the soil evasion flux system. The saturated mercury vapor was injected into the chamber through holes on the chamber wall. The mercury concentration was measured by the analyzer and the recovery rate of mercury was calculated with equation 3. In this study, the mercury

analysis system is regarded as providing accurate measurement within 80~120% recovery rate of the standard addition.

$$R = \frac{(C_{measured} - C_{ambient}) \times V_{measured} \times (v_{pump} + 1)}{C_{saturation} \times V_{injected}} \quad [3]$$

$C_{saturation}$ is the mercury saturation concentration at a given air temperature ($ng \cdot m^{-3}$);

$C_{measured}$ is the mercury concentration the 2537A analyzer detected ($ng \cdot m^{-3}$);

$C_{ambient}$ is the mercury concentration in ambient air ($ng \cdot m^{-3}$);

$V_{injection}$ is the volume of saturate mercury air injected in the sampling air flow (μL);

V_{sample} is the volume of sampling air measured by the 2537A analyzer (L); and

v_{pump} is the flow rate of GAST pump ($L \cdot min^{-1}$).

In this study, $C_{saturation}$ is obtained from mercury saturation concentration table base as a function of air temperature, V_{sample} is 5 L, and v_{pump} is 3.4 m/s.

2.4.4 Determining the GAST Pump Flux

To determine the flow rate of the GAST pump for use in field measurement of mercury flux, an experiment was conducted in the laboratory. The dynamic flux chamber was sealed on a Teflon board with plasticine. The saturated vapor of mercury was injected into the chamber through a hole on the chamber wall, the mercury concentration was measured by the 2537A mercury vapor analyzer, and the recovery rate was calculated with equation 3. In the experiment, the recovery rate was examined at three different flow rates (3, 3.4, 5.9 $L \cdot min^{-1}$). The injection was repeated 10 times at each flow rate. The result revealed that the mercury recovery rate

is most stable (108.0%±1.1%) at the GAST pump flow rate of 3.4 $L \cdot min^{-1}$.

2.5 Data Analysis

The mean value and standard deviation of the measurements for a particular period were calculated using data within the 90th confidential intervals of that period. The data were subdivided by season (winter: December-February, spring: March-May, Summer: June-August, and fall: September-November) and hours of day (Eastern Standard Time). The wind data were classified into 11 subsets based on wind speed, and average TGM concentrations were calculated for each subset. The Spearman's correlation coefficient was used in a bivariate correlation analysis. T-test and ANOVA test were used to examine differences in variables between two and among more groups, respectively. Linear regression was used to examine linear relationships between factors.

2.6 Data from Other Study Sites

Meteorological data were available from a weather station installed on the tower and operated by the State University of New York College of Environmental Science and Forestry (SUNY-ESF). These data include air temperature (1.8 m and 42.3 m), relative humidity, solar radiation, precipitation, wind speed and direction at 15-minute intervals. The air quality data from 2010 to 2012, included CO, SO_2 and O_3, were provided by US EPA at Madison, NY (N 43°05'24", W 76°05'92"). TGM data at the Syracuse CoE site were compared to values from other sites. These include a site operated by Dr. Huiting Mao located on the roof of Jahn Hall on the SUNY-ESF campus, which is approximately 25m above ground and located on the south of the

CoE site, 1.8 km away. Three other sites were examined that are associated with the National Atmospheric Deposition Program, Atmospheric Mercury Measurement Network, located in Rochester (NY95; N 43°8'46.67", W 77°32'53.20"), NY, Huntington Forest (NY20; N 43°58'23.16", W 74°13'23.16"), in the rural Adirondacks, and in the New York City (NY06; N 40°52'4.80", W 73°52'41.52").

Figure 4. Location of atmospheric mercury monitoring sites used in New York State.

3. Results

3.1 TGM Variations and Factors Controlling TGM Variation Prior to Soil Removal

3.1.1 Overall Summary

The average TGM concentrations at the Syracuse CoE from 2011 to 2012 were 1.6±0.58 and 1.4±0.40 ng/m^3 at the ground and upper levels, respectively (Table 1). The concentrations at the ground level were significantly higher than those at the upper level (Figure 5) during this period ($p<0.001$). Concentrations at the upper level generally increased with increasing TGM concentrations at the ground level (Figure 6). However, with increases in TGM concentrations at ground level, TGM concentrations at the upper level increased but to a lesser degree, resulting in a divergence in the relationship of the concentrations between the two heights ($y = 0.62 \cdot \ln x + 1.09$; where x is TGM concentrations at the ground level and y is the TGM concentration at the upper level; $p<0.01$).

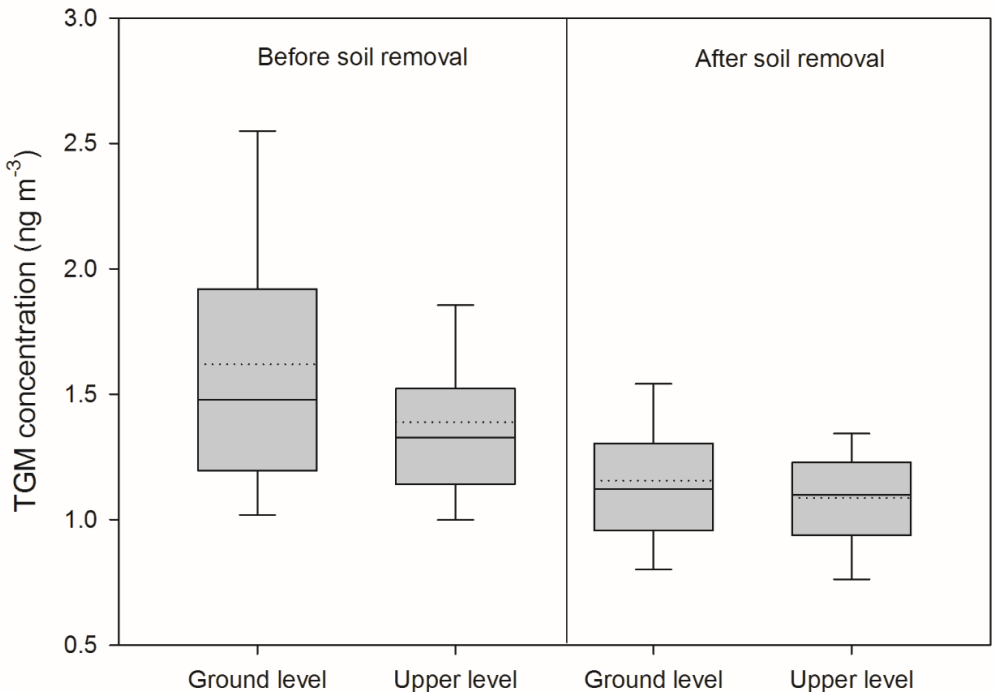

Figure 5. Comparison of overall average TGM concentrations for ground and upper level, and before (2011-2012) and after (2015-2016) brownfield remediation. Shown are the mean and median values, quartile range and extreme observations.

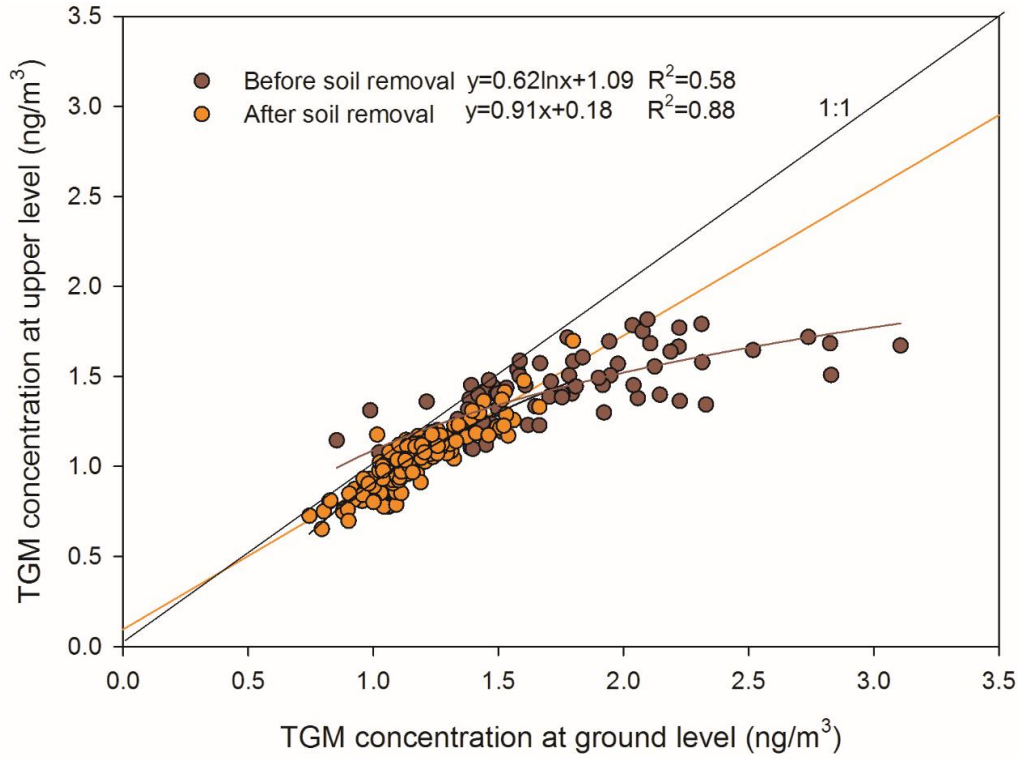

Figure 6. Comparison of TGM concentrations at the ground level with values at height before (2011-2012) and after soil removal (2015-2016).

3.1.2 Seasonal Variation

Seasonal average concentrations of TGM from 2011 to 2012 with associated meteorological and atmospheric chemical parameters are compared in Table 1. Seasonal average concentrations of TGM were 1.5±0.44, 1.8±0.55, 1.7±0.60 and 1.4±0.27 ng/m^3 at the ground level and 1.3±0.29, 1.5±0.32, 1.4±0.46, 1.3±0.27 ng/m^3 at the upper level, in spring, summer, fall, and winter, respectively. The maximum TGM concentrations at both heights occurred in summer, and minimum TGM concentrations occurred in winter. Meteorological parameters and air pollutants also exhibited seasonality, with maximum air temperature, solar radiation, precipitation and O_3 occurring in summer; maximum humidity, snowfall, CO, SO_2 occurring in winter; and maximum of CO_2 occurring in spring.

Table 1. Seasonal mean and standard deviation of TGM measurements and supporting meteorological factors, air quality concentrations at Syracuse for 2011-2012

	Spring	Summer	Fall	Winter
TGM concentration at ground level (ng/m^3)	1.5±0.44	1.8±0.55	1.7±0.60	1.4±0.27
TGM concentration at upper level (ng/m^3)	1.3±0.29	1.5±0.32	1.4±0.46	1.3±0.27
Temperature at ground level (℃)	10.34±7.60	23.10±4.80	9.01±5.26	1.95±4.80
Temperature at tower level (℃)	9.68±7.39	22.11±4.35	8.51±5.35	1.47±4.79
Solar radiation (W/m^2)	200.45±90.42	283.89±88.01	52.93±50.37	67.70±42.87
Daily average precipitation (mm)	1.04	4.49	3.49	2.50
Humidity (%)	59.83±19.84	59.16±16.39	66.35±17.71	71.29±15.46
Seasonal snowfall (cm)	55.7	0	25.1	233.8
CO (ppm)	0.28±0.10	0.27±0.07	0.31±0.16	0.32±0.15
CO_2 (ppm)	404.68±25.35	399.28±27.63	397.29±12.73	403.21±22.30
SO_2 (ppm)	0.55±0.67	0.62±0.69	0.71±0.64	0.82±0.69
O_3 (ppm)	0.03±0.01	0.04±0.02	0.02±0.01	0.02±0.01

3.1.3 Diurnal Variability

Different diurnal patterns of TGM concentration were observed for different seasons at ground level prior to brownfield remediation (Figure 7). In spring, TGM concentrations constant at night, increased and reaching a maximum at 10:00, decreased until sunset, then increased in early evening. In summer, TGM concentrations increased starting in early afternoon reaching a peak at midnight, followed by another increase at sunrise and reaching a maximum in early morning and then values decreased until early afternoon. In fall, TGM concentrations increased after sunrise and reaching a peak at noon, followed by a decrease in the afternoon, which reversed after sunset reaching a peak before midnight. In winter, TGM maintained a low and relatively constant concentration during nighttime, followed by an increase in the morning reaching a maximum at 14:00, with values decreasing in the afternoon to the evening. At the upper height, the diurnal patterns in non-winter seasons were similar with diurnal patterns at the ground level. In the winter relatively constant TGM concentrations were observed throughout the day.

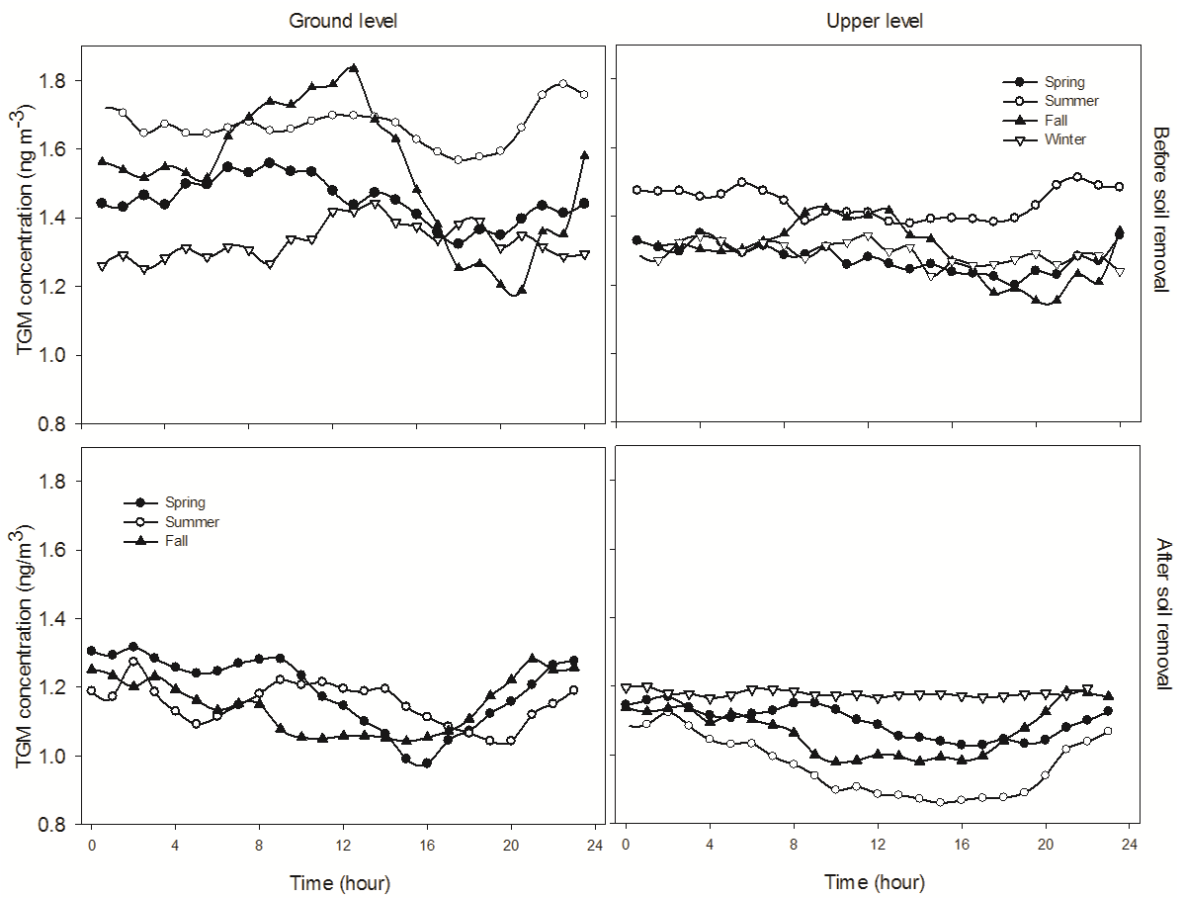

Figure 7. Comparison of diurnal patterns of TGM concentration at ground level and height before (2011-2012) and after brownfield remediation (2015-2016).

3.1.4 Relationships between TGM Concentrations and Meteorological Factors

The daily average TGM concentrations were positively related with daily average air temperatures at the two heights prior to brownfield remediation (Figure 8; TGM concentration (y, in $\text{ng} \cdot m^{-3}$) and air temperature (x, in ℃) is $y = 1.31 + 1.97\times10^{-2}x$ ($p<0.01$) at the ground level and $y = 1.17 + 1.19\times10^{-2}x$ ($p<0.01$) at upper level, respectively).

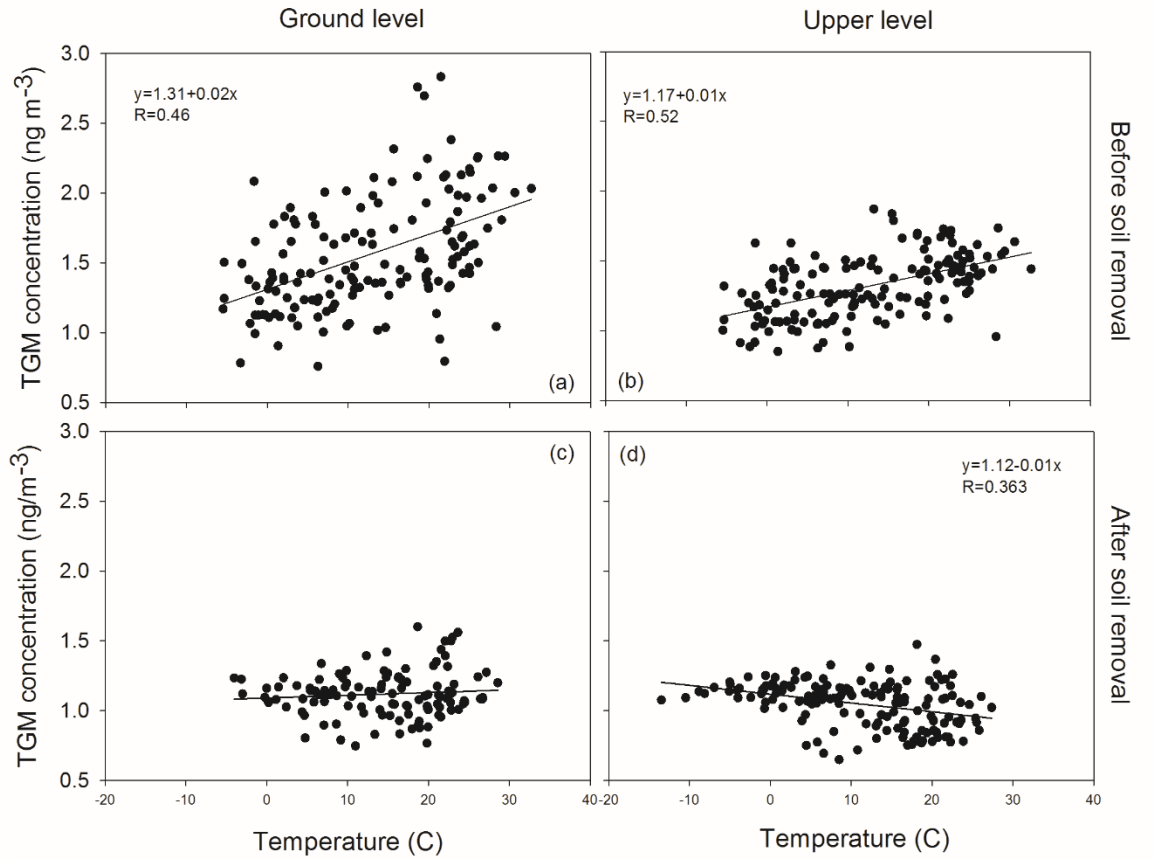

Figure 8. Relationship between TGM concentration and air temperature at ground level and at height before (2011-2012) and after (2015-2016) brownfield remediation.

The daily average TGM concentrations were positively related with daily average solar radiation at both heights prior to brownfield remediation (Figure 9; $y = 1.25 + 1.5\times10^{-3}x$ at the ground level and $y = 1.13 + 1\times10^{-3}x$ at upper level, where y is TGM concentration ($ng \cdot m^{-3}$) and x is solar radiation (W/m^2)).

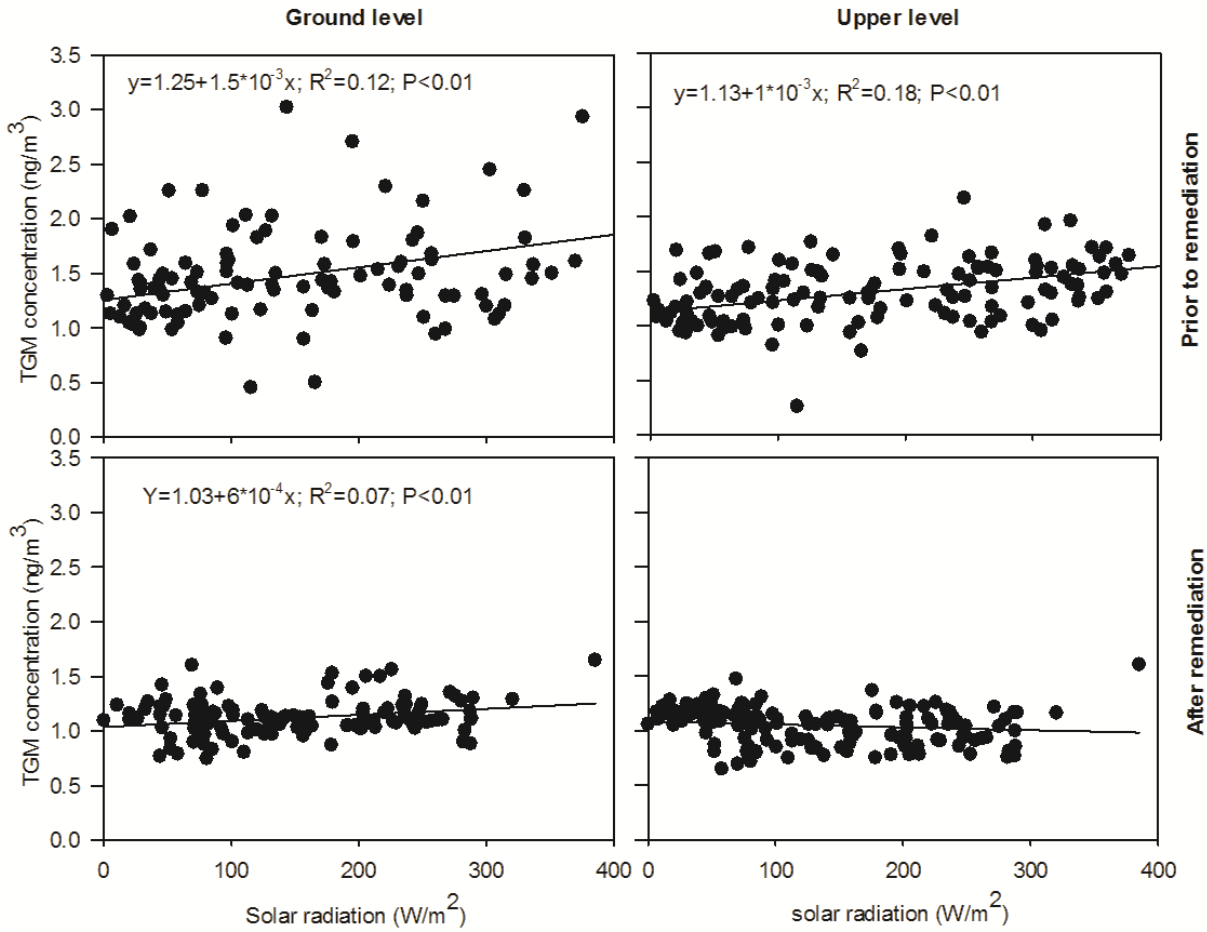

Figure 9. Comparison of TGM concentrations and solar radiation at ground and upper level before (2011-2012) and after (2015-2016) brownfield remediation.

TGM concentrations were negatively related to wind speeds at both heights prior to soil remediation. TGM concentrations decreased markedly with increasing wind speed at low wind speeds (<7m/s), and approached a relatively constant concentration with increasing wind speed (Figure 10a; $y = 1.85 - 0.26 \cdot \ln x$; $p<0.01$ at the ground level and $y = 1.45 - 0.13 \cdot \ln x$; $p<0.01$ at the upper level, where y is TGM

concentration ($ng \cdot m^{-3}$) and x is wind speed (m/s)).

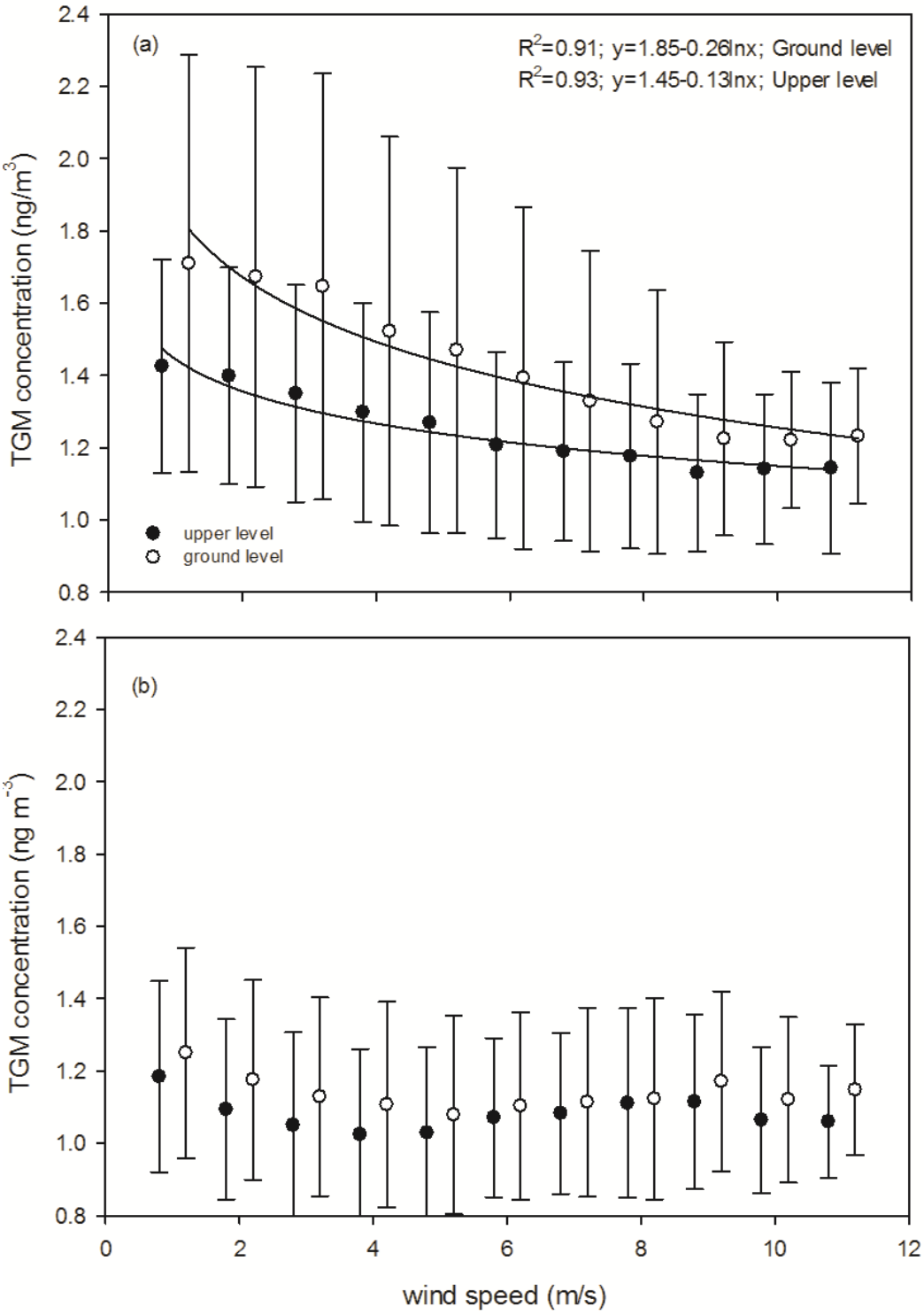

Figure 10. Comparison of relationship between TGM concentrations and wind speed at height before (2011-2012) and after (2015-2016) brownfield remediation.

3.2 TGM Variations and Controlling Factors after brownfield Removal

3.2.1 TGM Variation

After brownfield soil removal and parking lot installation, there was a significant decrease in TGM concentrations observed at both heights. The average TGM concentration after soil removal (2015-2016) were 1.1 ± 0.28 and 1.1 ± 0.24 ng/m^3 at the ground level and upper level, respectively. There was no significant difference between TGM concentrations at two heights (Figure 5). The relationship of TGM concentrations at the ground level (X) and the TGM concentration at upper level (Y) is $y = 0.91x + 0.18$ ($p<0.01$).

After brownfield remediation, diurnal patterns were significantly altered. At the ground level, TGM concentrations increased at nighttime and decreased to lower values during daytime, then increasing after sunset in the spring and fall. In summer, TGM increased after sunset and reaching a maximum at 2:00, followed by a decrease to early morning, and then concentrations increased and remaining elevated until noon. There were no data collected at ground level in winter due to instrument failure. At the upper level, TGM had higher concentrations at nighttime and decreased to lower concentrations during daytime in non-winter seasons, but remained constant concentration throughout the day in winter.

3.2.2 Relationship between TGM Concentrations and Meteorological Factors

After brownfield remediation, there was no relationship between daily average TGM concentration and air temperature at the ground level (Figure 8c), but a negative linear relationship became evident at the upper height (Figure 8d; TGM concentration

(y, in $ng \cdot m^{-3}$) and air temperature (x, in ℃) is $y = 1.12 - 0.01x$ (p<0.01)). A weak positive correlation between TGM concentrations and solar radiation was observed at the ground level (Figure 9; TGM concentration (y, in $ng \cdot m^{-3}$) and air temperature (x, in W/m^2) is $y = 1.03 + 6\times10^{-4}x$). No significant correlation between TGM concentrations and solar radiation was observed. In addition, no relationships were detected between TGM concentrations and wind speed (Figure 10b) after soil removal and parking lot installation.

3.2.3 Relationship of Mercury Evasion Flux with TGM Concentrations and Meteorological Factors

Soil mercury evasion flux was measured at the CoE in June 2015 after remediation (Figure 11a). The net daily mercury flux was negative (-1.72 $ng \cdot m^{-2} \cdot day^{-1}$; net deposition) for the month. Mercury flux was negative value during nighttime (i.e. net deposition). Values sharply increased at 5:00 and reached a maximum at 8:00, remained as net emission to the atmosphere until 12:00 and then decreased to negative values. This flux pattern positively related to the diurnal pattern of TGM concentration at the ground level for this month (R=0.71, P<0.01). Moreover, soil mercury flux measurements were correlated with air temperature (R=0.54, p<0.01), solar radiation (R=0.83, p<0.01), UV radiation (R=0.71, P<0.001), visible light (R=0.71, P<0.001), IR radiation (R=0.73, P<0.001) and ground temperature (R=0.48, P<0.05).

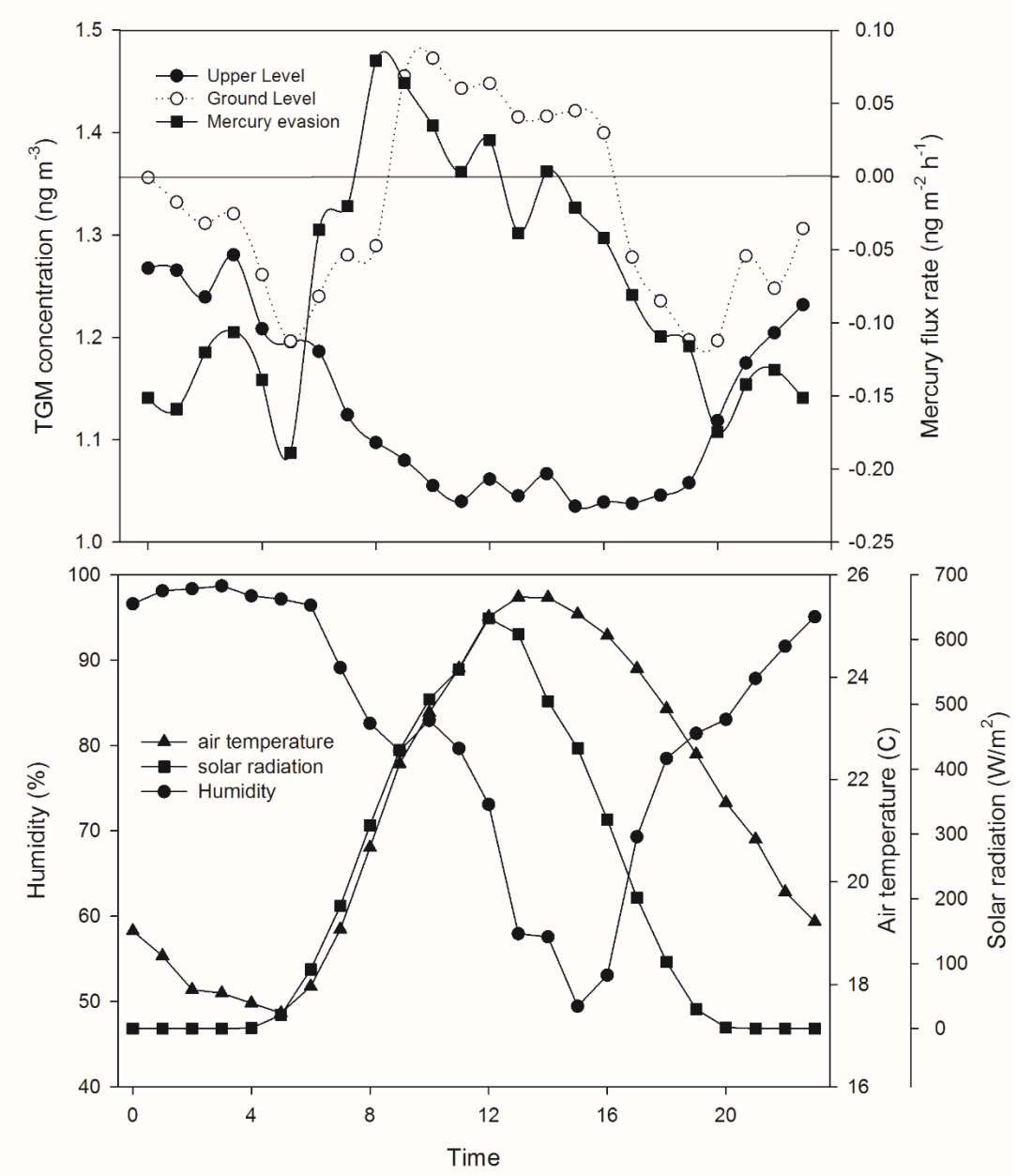

Figure 11. Mean daily diurnal pattern of TGM concentrations at the ground level and at height with mercury evasion flux from soil in June 2015. Also shown are air temperature, solar radiation and relative humidity.

4. Discussion

4.1 TGM Variation Prior to Soil Removal

4.1.1 Meteorological Factors Influence on TGM Concentrations

Daily average TGM concentrations were positively correlated with air temperature at both heights before soil remediation and parking lot installation (Figure 8). This observation is consistent with study of Zhu et al. (2012) of an urban site in Nanjing, China and suggests that TGM concentrations are controlled by local soil mercury evasion which increases with increasing air temperature (Gabriel et al., 2006). The increasing rate of TGM concentration with air temperature was different for the two heights, the rate at the ground level (0.02 $ng \cdot m^{-3} \cdot ℃^{-1}$) was twice that at the upper height from the land surface (0.01 $ng \cdot m^{-3} \cdot ℃^{-1}$). The difference of increasing rate of TGM concentration with air temperature at the two heights is likely due to the dilution of surface mercury with the surrounding air. Zhu et al. (2012) reported a 0.17 $ng \cdot m^{-3} \cdot ℃^{-1}$ TGM increasing rate with air temperature at urban area of Nanjing, almost an order of magnitude greater than these observed at the CoE. Very high mercury TGM concentrations (7.9±7.0 ng/m^3) in ambient air were reported for the Nanjing study and elevated mercury concentration undoubtedly contributes to the difference in the mercury sources between the two sites.

A positive relationship between TGM concentration and solar radiation was observed in this study, which may reflect enhanced mercury emission rate with solar radiation (Gustin et al., 2002). However, TGM concentration had moderate correlation

with solar radiation, which may because of GEM oxidation also increases with increases in solar radiation (Poissant et al., 2004), which could offset the enhancing effect of solar radiation on mercury emission rate.

Negative correlations between TGM concentrations and wind speed were observed at both heights (Figure 10a). At low wind speed, TGM concentrations decreased markedly with increasing wind speed. With increases in wind speed TGM concentration decreased and eventually leveled off. Gabriel et al. (2006) reported mercury evasion from bare soil is much higher than that from impervious surfaces. Therefore, TGM concentrations at the CoE site was likely higher than the surrounding air due to soil mercury evasion from the brownfield soil. The negative relationship between wind speed and TGM concentration is thought to be the result of local TGM supplied from emission of brownfield soil that was diluted by cleaner air entering the site from surrounding area (Lan et al., 2014). TGM approached a constant concentration (1.2 ng/m^3) at upper level at higher wind speeds, which are thought to approach concentrations of ambient air (NY20; Table 2).

Table 2. Annual mean and standard deviation of TGM for Syracuse COE and other sites in New York (2011-2016)

		NY06	NY20	NY95	Syracuse Ground	Syracuse upper
2011-2012	Overall	1.6±0.40	1.3±0.29	1.4±0.32	1.6±0.58	1.4±0.40
	spring	1.5±0.33	1.5±0.26	1.3±0.18	1.5±0.44	1.3±0.29
	summer	1.6±0.38	1.20±0.30	1.3±0.21	1.8±0.55	1.5±0.32
	fall	1.6±0.57	1.2±0.30	1.4±0.54	1.7±0.60	1.4±0.46
	winter	1.5±0.27	1.3±0.14	1.4±0.15	1.4±0.27	1.3±0.27
2015-2016	Overall	1.8±0.27	1.2±0.22	1.4±0.20	1.1±0.28	1.1±0.24
	Spring	1.8±0.25	1.3±0.11	1.4±0.16	1.2±0.20	1.1±0.12
	Summer	1.8±0.33	1.1±0.22	1.4±0.27	1.1±0.31	1.0±0.28
	Fall	1.7±0.30	1.1±0.21	1.3±0.18	1.1±0.26	1.0±0.27
	winter	1.8±0.27	1.3±0.11	1.3±0.22	------	1.2±0.10

4.1.2 Vertical TGM Concentration Differences

TGM concentrations at the ground level were significantly higher than those at height prior to brownfield remediation, and the difference in concentration between the two heights increased with increasing TGM concentrations (Figure 5). This divergence in concentrations with elevation is thought to be due to mixing and dilution with ambient air with lower TGM concentrations. TGM concentrations at the CoE showed seasonal differences, with the highest values in summer and the lowest concentrations in winter. This seasonal variation in TGM concentration is thought to be a result of mercury emissions from the land surface which is enhanced with increases in temperature and solar radiation (Kim et al., 2011; Lan et al., 2014; Zhu et al., 2012). TGM emissions from the local ground surface appears to be an important mercury source at this site. Some of the TGM at the upper height is likely derived from the local ground surface which was vertically transported to a higher elevation.

4.1.3 The Diurnal Variation of TGM Concentrations

Different diurnal patterns were observed at the two heights in different seasons, which is thought to be a result of seasonal variation in PBL height, mercury emissions from the ground surface, GEM oxidation and dilution.

In spring, similar diurnal patterns were evident at the two heights. TGM reached maximum at sunrise, then decreased until the sunset. This pattern is frequently reported in urban areas and thought to primarily due to the variation in PBL height (Choi et al., 2013; Lan et al., 2014; Song et al., 2009). The PBL maintains a low height at nighttime,

limiting TGM dilution with the upper atmosphere. Under a low PBL height with constant anthropogenic mercury release, TGM accumulates and its concentrations increase. After sunrise, PBL height increases with air temperature (Figure 12). The increase in PBL height allows surface air mixing with air away from the Earth's surface decreasing TGM concentrations. In addition, increased temperature and solar radiation could enhance GEM oxidation during daylight, which would also decrease TGM concentrations.

In summer, TGM concentrations increased during nighttime and reaching a peak at midnight, followed by an increase at sunrise reaching a maximum at 8:00 and then decreased. The nocturnal increase in TGM concentration is thought to due to decrease in the PBL height as suggested above. The increase in TGM concentration at sunrise is likely to be a result of an overnight accumulation, however, the decrease in TGM concentration observed in the early morning contrasts with this hypothesis. There are two possible explanations for the increase in TGM at sunrise. Stamenkovic et al. (2007) explained this increase as reemission of mercury deposited to the ground surface during nighttime with daylight increases in solar radiation; Scheroeder et al. (1998) interpreted this increase as TGM in the upper atmosphere above the residual layer mixing with surface air associated with an increase in the PBL height after residual layer eroded. TGM concentrations in fall were similar with those in summer, however, the increase at sunrise was not observed (Figure 7). This difference suggests that TGM from upper atmosphere mixing with surface air is not the mechanism for the increase in TGM concentration during summer, but rather mercury reemissions associated with solar

radiation. Solar radiation is weakened in fall (Table 1), resulting in less TGM emitted at sunrise, limiting the TGM increase observed at sunrise. TGM concentrations remained constant concentration during daylight in summer, which is likely a result of mercury evasion from the brownfield offset by mercury loss due to increasing GEM oxidation and mercury dilution with increasing PBL height.

In fall, TGM concentrations increased after sunrise, reaching a maximum at noon then decreased until sunset. This pattern is thought to be a result of TGM increases due to reduced PBL height during night and strong mercury emission from the ground surface in the morning. Decreases in the afternoon are likely due to increasing GEM oxidation and RGM deposition. TGM concentration increases due to local mercury evasion tend to offset by GEM oxidation, however solar radiation is weakened in fall, and mercury evasion exceeds GEM oxidation causing TGM concentrations to increase in the morning.

During winter, the diurnal patterns were different at the two heights. At the ground level, TGM concentrations increased from 9:00 to 14:00, then decreased and remained low concentration for the remainder of the day. At the upper height, a constant concentration of TGM was maintained throughout the day. There was no nocturnal increase in TGM concentration observed at the two heights. Low air temperature and snowpack are probably responsible for the lack of nocturnal TGM increase. Gabriel et al. (2006) showed that soil mercury flux is significantly related with air temperature. Low air temperature likely limits soil mercury evasion. Moreover, the ground surface at this site is covered with snow for extended periods during winter. Any TGM emitted

from ground surface was likely trapped by snowpack. These two factors likely limit soil TGM emission rate during winter and as a result TGM concentrations remained low during nighttime. After sunrise, mercury evasion increased with increasing air temperature, possibly associated with the release of TGM from melting snow (Choi et al., 2013; Huang et al., 2010). This hypothesis is supported by the correlation between diurnal pattern of TGM concentration at the ground level with air temperature (0.93, $p<0.01$). Due to mixing, the released TGM from melting snow was diluted with ambient air and did not reach the upper height, causing TGM concentrations at upper height to remained at a constant concentration.

4.2 Brownfield Influence on TGM Concentrations and Variation

4.2.1 Brownfield Influence on TGM Concentrations

After soil removal and parking lot installation, there were 32% and 22% decreases in TGM concentrations observed at the ground and upper level, respectively. The remarkable decrease in TGM concentration is thought to be due to a reduction in local mercury emissions associated with brownfield restoration. Regional decreases in TGM concentrations associated with emission controls might also be a factor. TGM measurements conducted from 2013-2015 at SUNY-ESF by Dr. Huiting Mao showed a 9% decrease in TGM concentration. The decrease in TGM concentrations is likely a representative of regional decrease. The decline rate at the ESF site much less than that at the CoE site, suggesting regional decrease in TGM concentration is not enough to explain the concentration decrease observed at the CoE site. It appears that brownfield

remediation is largely responsible for the decrease in TGM concentrations at the CoE site.

The brownfield is thought to elevate local TGM concentrations due to enhanced local mercury evasion. TGM concentrations were positive correlated with air temperature (Figure 8) and solar radiation (Figure 9) prior to brownfield remediation. These relationships provide evidence that local mercury evasion drives the magnitude and some of the variation in local TGM concentrations. These correlations were not evident after remediation, suggesting that local soil evasion was a much smaller contribution to local TGM concentrations after brownfield remediation. Indeed, mercury flux measurements in summer after brownfield remediation (Figure 8) showed a net deposition of TGM to this site (-1.72 $\text{ng} \cdot m^{-2} \cdot day^{-1}$). Moreover, TGM concentrations did not vary with wind speed (Figure 10b) after brownfield remediation.

The concentrations difference between the two heights was caused by the relatively high local soil mercury evasion coupled with dilution following vertical transport from the land surface, as suggestion in section 4.1.2. However, mercury from regional air was the dominate source after brownfield remediation. The concentration data in Table 2 does not indicate this. There was no TGM concentrations difference between the two height after remediation (Table 1).

Prior to remediation, TGM diurnal patterns were significant affected by local mercury evasion and variation in PBL height. The two factors caused TGM concentrations to be elevated during night and in the morning. After remediation, the influence of soil mercury evasion was reduced and PBL variation became the dominate

influencing factor. A diurnal pattern, which had higher TGM concentrations during nighttime and lower during daytime was observed during the non-winter seasons at the upper level and in spring and fall at ground level. Even though the influence of mercury evasion reduced after brownfield remediation, however, it still significantly promoted TGM concentration at the ground level in summer due to increasing mercury reemission with higher air temperature and stronger solar radiation.

4.2.2 Influence on Relationship between TGM Concentration and Meteorological Factors

The role of brownfield mercury emissions on local TGM concentrations is also demonstrated by the change of relationships between TGM concentrations and meteorological factors. Prior to brownfield removal, the daily average TGM concentrations were positive related with daily average air temperature (Figure 8a, 8b), however, there was no relationship with air temperature at the ground level (Figure 8c) and a negative relationship at the upper level (Figure 8d) after brownfield remediation. The change in the TGM-temperature relationships is thought to be a result of reduced local mercury emission due to brownfield removal. Air temperature affects TGM concentrations through several mechanisms: Increasing air temperature promotes mercury emission. At same time, increasing air temperature also speeds up GEM oxidation rate and enhances TGM dilution associated with increasing PBL height. Prior to brownfield remediation, TGM released from soil mercury emission exceeded TGM losses due to dilution and oxidation. The overall net effect was increased local TGM concentrations, which resulted in a positive relationship between TGM concentration

and air temperature. After soil remediation, mercury emission decreased and TGM was likely derived from regional sources. At the upper level, mercury supply from local evasion was reduced but was ongoing losses from oxidation and dilution remain constant, causing a negative relationship between TGM and air temperature (Figure 8d). At the ground level, loses from oxidation and dilution exceeded mercury evasion in spring and fall, which likely caused a negative correlation between air temperature and TGM concentration. However, enhanced mercury evasion due to high air temperature and strong solar radiation were greater than the loses in summer, resulting in a positive relationship between air temperature and TGM concentration. Considering all observations, following soil remediation TGM concentrations did not vary with air temperature (Figure 8c).

Solar radiation is thought to accelerate GEM oxidation, and induce deposited mercury to be reduced and re-emited. The positive correlations between TGM concentration and solar radiation prior to brownfield remediation should be the result of enhanced mercury evasion exceeding mercury loss due to GEM oxidation. After brownfield remediation, TGM concentrations decreased resulting in less TGM deposited to the ground surface and less TGM reemitted due to solar radiation. Thus, the increasing effect of solar radiation on TGM concentrations reduced, and is offset by GEM oxidation, resulting in TGM concentrations that did not vary with solar radiation after brownfield remediation (Figure 9).

Wind is thought to decrease local TGM concentrations by advecting cleaner air into this site as discussed in section 4.1.1, causing negative correlations between TGM

concentration and wind speed. However, TGM approached a constant concentration (1.2 ng/m^3) at the upper level with higher wind speeds, which approximately the regional concentration value (NY20; Table 2). Since TGM concentrations at the COE did not vary with wind speed after brownfield, local TGM concentration (1.1 ng/m^3) should be representative of regional ambient concentrations, which is considered as a concentration with air well mixing at Syracuse urban area. There was a 2.1%/year decrease in regional TGM concentrations, which is consisted with the decline rate observed at Huntington Forest (1.9%/year) at same time period, demonstrating my hypothesis in Section 4.2.1 that the decrease in TGM concentration observed after soil remediation was the result of brownfield removal rather than a decrease in regional TGM concentration.

4.3 Comparison with Mercury Variation at Other Sites

4.3.1 The Comparison with Mercury Study in Toronto

In this study, a decrease in TGM concentrations with increasing height of the sampling air inlet was evident prior to brownfield removal but concentrations were similar at both heights after soil removal. Mercury studies conducted at Toronto showed a positive relationship between GEM concentrations and the height of sampling inlets from the ground surface. Observations from Toronto showed GEM concentrations were 2.39±2.05 ng/m^3 at 3.5 m, 2.57±2.39 ng/m^3 at 7 m (Denis et al., 2006) and 4.5±3.1 ng/m^3 at 12 m (Song et al., 2009) above the land surface. The 7 m air inlet was positioned in the tree canopy layer and the 3.5 m inlet was positioned under the canopy

layer. The tree canopy is thought to affect the vertical patterns of GEM concentrations. It is hypothesized that TGM concentration at 12 m is representative of ambient air. The lower TGM concentrations at lower heights beneath the tree canopy are thought to be due to mercury retention by foliage.

4.3.2 Comparison of TGM Variation at the CoE with Other Sites in NY State

The overall average TGM concentration from 2011 to 2012 were 1.6±0.40, 1.3±0.29 and 1.4±0.32 ng/m^3 for Bronx (NY06), Huntington Forest (NY20) and Rochester (NY95), respectively. A comparison of TGM concentrations at AMN sites with the observations in Syracuse showed that the ground level at Syracuse had the highest concentrations among the sites, followed by Bronx, Rochester, upper height at Syracuse and Huntington Forest. Huntington Forest is the only rural site and had the lowest TGM concentrations of the study sites, suggesting that local anthropogenic mercury sources contributed to higher TGM concentration in urban areas. Syracuse and Rochester are at similar latitudes, but TGM concentrations at the ground level at Syracuse prior to brownfield restoration were higher than concentrations at Rochester. The upper level at Syracuse had similar TGM concentrations as Rochester again suggesting that emissions from the brownfield were contributing to elevated TGM at Syracuse.

Different diurnal patterns were observed across the seasons at the AMN sites (Figure 12). At Bronx and Rochester, different diurnal patterns were observed during winter and non-winter periods. In winter, the TGM concentrations remained at a

constant concentration through the day. During non-winter seasons, TGM concentrations were higher at nighttime and decreased to lower values during daytime. The variation in the PBL height is considered as the primary factor for diurnal variation in TGM during the non-winter seasons. Reduced mercury emissions associated with cold weather conditions and snowpack caused TGM remain at low and constant concentrations at the two sites during winter.

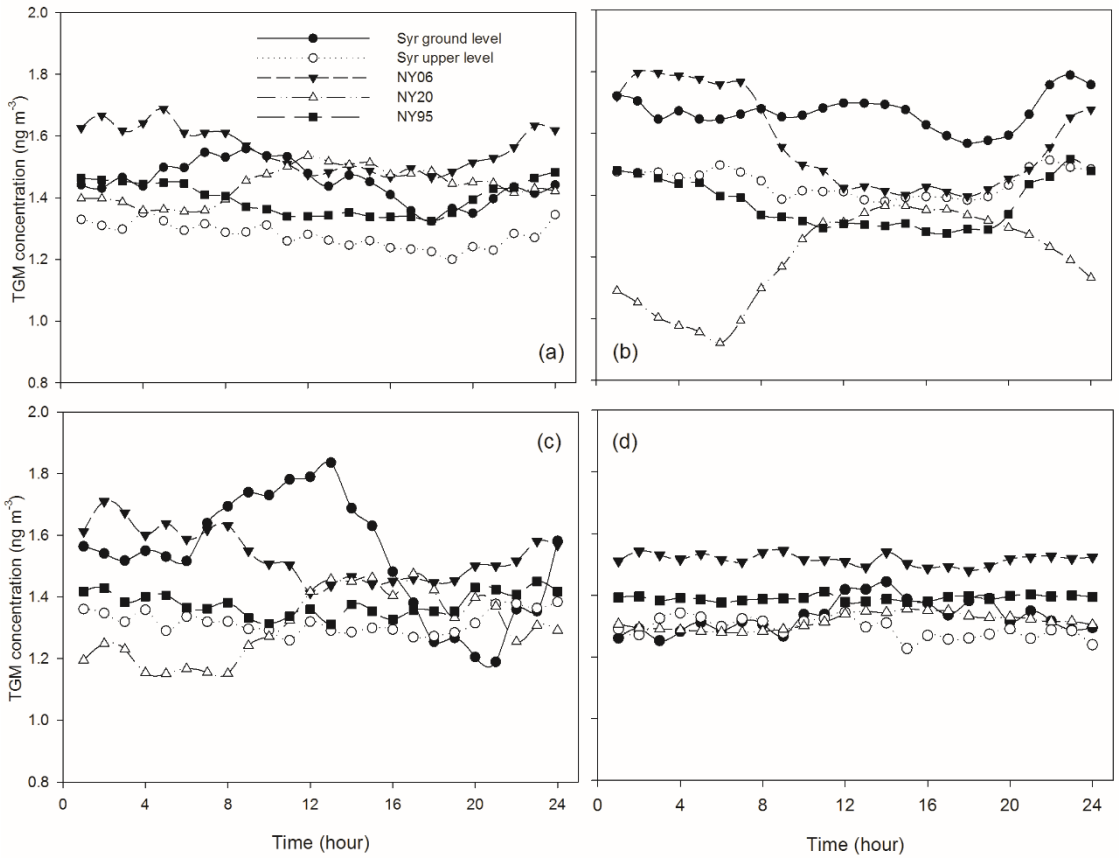

Figure 12. Comparison of TGM diurnal patterns for Syracuse with AMN sites in New York State, including (a) spring; (b) summer; (c) fall; and (d) winter (2011-2012).

At Huntington, different diurnal patterns were observed during winter and non-winter periods. In winter, the TGM concentrations remained constant at night, follow by an increase in TGM concentration in the afternoon. In the non-winter seasons, TGM concentrations reached a minimum value before sunrise, then increased and reached a maximum value around noon, and concentrations decreased in the afternoon until the next sunrise. The non-winter patterns are similar to patterns reported for rural areas and are thought to be driven by soil mercury evasion (Choi et al., 2013; Kellerhals et al., 2003; X. Lan et al., 2012). In winter, snowpack and cold weather limits mercury evasion and the increases in TGM concentrations in the morning were not evident. In the afternoon, TGM release by evasion from either bare soil due to increasing air temperature, or associated with TGM release from melting snow caused an increase in TGM concentration.

A diurnal pattern, which has higher TGM concentration during night and lower concentration during daylight, was frequently observed at the CoE site after brownfield remediation. This pattern consistent with the diurnal patterns observed at the Bronx and Rochester during non-winter seasons. This consistency suggests a common diurnal pattern of TGM concentrations in urban areas in NY State and indicates the diurnal patterns at the CoE site prior to brownfield removal were influenced by local mercury emissions. The winter pattern at the ground level of CoE site was similar with the winter pattern at Huntington Forest, which is thought to be due to cold weather associated with mercury release from melting snow. The winter pattern at the upper level at COE was similar to winter pattern observed at the Bronx and Rochester, which is considered a

result of cold weather associated with reduced soil mercury emissions. The difference in winter patterns between the two heights may be the result of mercury released from melting snow diluted to ambient air through vertical transport.

Among the five site, Huntington Forest is the only rural site that did not exhibit a nocturnal TGM increase during any season. Nocturnal TGM increases were observed at the urban sites in the non-winter seasons, but not in winter. Since Huntington Forest is the only rural monitoring site, mercury emissions were likely reduced after sunset with decreasing air temperature and solar radiation (Choi et al., 2013). Urban sites had lower local mercury emission rate in winter due to cold weather and snow cover. Therefore, the lack of nocturnal TGM increases during winter are likely a result of low mercury emission rate at nighttime. However, there is not enough evidence to prove this hypothesis.

5. Conclusions

In this study, TGM variations at an urban brownfield were measured at two different heights from the land surface. Prior to brownfield remediation, TGM concentration and its diurnal and seasonal variations were significantly different at the two heights. Concentrations at the ground level were significant higher than those at the upper level and the concentrations difference between the two heights increased with increasing TGM concentration at ground level. The highest average concentrations were observed in summer and lowest concentrations were observed in winter.

Multiple factors are thought to affect TGM variation at the Syracuse CoE site. Mercury emissions from the ground surface is thought to have been a substantial as

mercury source at this site. The extent of mercury evasion likely varied with season, with the highest rate in summer and lowest in winter. The variation in PBL height also influenced TGM diurnal variation at this site. The reduced PBL height at nighttime caused TGM concentrations to increase, and the increased PBL height during daytime coupled with elevated GEM oxidation, deposition and dilution likely caused TGM concentrations to decrease.

TGM variation in urban areas has been reported to be significantly influenced by variation in PBL height, however few studies have reported the influence of seasonal variation in soil mercury evasion. There was a brownfield adjacent to the CoE site, and evasion of mercury from brownfield soil is thought to be a major factor causing elevated TGM concentration before soil remediation. During remediation, the contaminated soil was removed and a parking lot installed adjacent to the site. The marked decrease in TGM concentrations, changes in diurnal patterns of TGM concentration, and changes in the relationships of TGM concentrations with meteorological factors suggests reduced local mercury evasion.

6. Suggestions for Future Study

In this study, interesting patterns of TGM concentration were observed in the Syracuse urban landscape. I have further questions which could be answered with additional research:

(1) There are limited TGM measurements after soil removal. In particular winter TGM measurements would provide information about TGM variation and changes after brownfield remediation.

(2) The influence of PBL height on TGM concentrations was recognized, but its impact was not quantified. To quantify the influence of PBL variation on TGM concentrations, information in mercury deposition rates and soil emission rates are needed. Mercury flux estimates are the net result of deposition and emissions. Combining TGM concentration and mercury flux measurement could be conducted to quantify the influence of the PBL on TGM variation.

(3) In order to improving understanding of the factors influencing variation in TGM concentrations and to be able to predict mercury concentration in the future, an atmospheric mercury model should be applied to the study site considering soil mercury emission rates, deposition rate, mixing rate due to vertical movement of the PBL and other influencing factors.

Reference

Amos, H. M., Jacob, D. J., Streets, D. G., & Sunderland, E. M. (2013). Legacy impacts of all‐time anthropogenic emissions on the global mercury cycle. *Global Biogeochemical Cycles, 27*(2), 410-421.

Bernhoft, R. A. (2012). Mercury toxicity and treatment: A review of the literature. *Journal of Environmental and Public Health, 2012, 460508-10.*

Buckley, S. M., Mitchell, M. J., McHale, P. J., & Millard, G. D. (2014). Variations in carbon dioxide fluxes within a city landscape: Identifying a vehicular influence. *Urban Ecosystems*, *19*(4), 1479-1498.

Choi, H.-D., Huang, J., Mondal, S., & Holsen, T. M. (2013). Variation in concentrations of three mercury (Hg) forms at a rural and a suburban site in New York State. *Science of the Total Environment*, *448*, 96–106.

Denis, M. S., Song, X., Lu, J. Y., & Feng, X. (2006). Atmospheric gaseous elemental mercury in downtown Toronto. *Atmospheric Environment*, *40*(21), 4016–4024.

Dommergue, A., Barret, M., Courteaud, J., Cristofanelli, P., Ferrari, C. P., & Gallée, H. (2012). Dynamic recycling of gaseous elemental mercury in the boundary layer of the Antarctic Plateau. *Atmospheric Chemistry and Physics*, *12*(22), 11027–11036.

Driscoll, C. T., Mason, R. P., Chan, H. M., Jacob, D. J., & Pirrone, N. (2013). Mercury as a global pollutant: Sources, pathways, and effects. *Environmental Science & Technology, 47*(10), 4967.

Ericksen, J. A., Gustin, M. S., Lindberg, S. E., Olund, S. D., & Krabbenhoft, D. P. (2005). Assessing the potential for re-emission of mercury deposited in precipitation from arid soils using a stable isotope. *Environmental Science & Technology*, *39*(20), 8001–8007.

Ehrlich, H. L and Newman D. K. (2008). Geomicrobiology. CRC Press. P. 265. ISBN 978-0-8493-7906-2.

Holmes, C. D., Jacob, D. J., Corbitt, E. S., Mao, J., Yang, X., Talbot, R., & Slemr, F. (2010). Global atmospheric model for mercury including oxidation by bromine atoms. *Atmospheric Chemistry and Physics*, *10*(24), 12037–12057.

Huang, J., Choi, H.-D., Hopke, P. K., & Holsen, T. M. (2010). Ambient mercury sources in Rochester, NY: results from principle components analysis (PCA) of mercury monitoring network data. *Environmental Science & Technology*, *44*(22), 8441–8445.

Impey, G. A., Shepson, P. B., Hastie, D. R., Barrie, L. A., & Anlauf, K. G. (1997). Measurements of photolyzable chlorine and bromine during the Polar Sunrise Experiment 1995. *Journal of Geophysical Research: Atmospheres*, *102*(D13),

16005–16010.

Keeler, G., Glinsorn, G., & Pirrone, N. (1995). Particulate mercury in the atmosphere: its significance, transport, transformation and sources. *Water, Air, and Soil Pollution*, 80 (1):159-168.

Kellerhals, M., Beauchamp, S., Belzer, W., Blanchard, P., Froude, F., Harvey, B., Puckett, K. (2003). Temporal and spatial variability of total gaseous mercury in Canada: results from the Canadian Atmospheric Mercury Measurement Network (CAMNet). *Atmospheric Environment*, *37*(7), 1003–1011.

Kim, K. H., Shon, Z. H., Nguyen, H. T., Jung, K., Park, C. G., & Bae, G. N. (2011). The effect of man made source processes on the behavior of total gaseous mercury in air: A comparison between four urban monitoring sites in Seoul Korea. *Science of the Total Environment*, *409*(19), 3801–3811.

Lan, X., Talbot, R., Castro, M., Perry, K., & Luke, W. (2012). Seasonal and diurnal variations of atmospheric mercury across the US determined from AMNet monitoring data. *Atmospheric Chemistry and Physics*, *12*(21), 10569–10582.

Lan, X., Talbot, R., Laine, P., Lefer, B., Flynn, J., & Torres, A. (2014). Seasonal and diurnal variations of total gaseous mercury in Urban Houston, TX, USA. *Atmosphere*, *5*(2), 399–419.

Lin, C., & Pehkonen, S. O. (1997). Aqueous free radical chemistry of mercury in the presence of iron oxides and ambient aerosol. *Atmospheric Environment*, *31*(24), 4125–4137.

Lindberg, S., Bullock, R., Ebinghaus, R., Engstrom, D., Feng, X., Fitzgerald, W., Seigneur, C. (2007). A synthesis of progress and uncertainties in attributing the sources of mercury in deposition. *Ambio*, *36*(1), 19–32.

Nozaki, K.Y. (1973) Mixing Depth Model Using Hourly Surface observation, Report 7053, USAF Environmental Technical Applications Center.

Parsons, M., McLennan, D., Lapalme, M., & Mooney, C. (2013). Total gaseous mercury concentration measurements at Fort McMurray, Alberta, Canada. *Atmosphere*, *4*(4), 472-493.

Petersen, G., Iverfeldt, Å., & Munthe, J. (1995). Atmospheric mercury species over central and northern Europe. Model calculations and comparison with observations from the Nordic air and precipitation network for 1987 and 1988. *Atmospheric Environment*, *29*(1), 47–67.

Poissant, L., & Casimir, A. (1998). Water-air and soil-air exchange rate of total gaseous mercury measured at background sites. *Atmospheric Environment*, *32*(5), 883–893.

Poissant, L., Pilote, M., Beauvais, C., Constant, P., & Zhang, H. H. (2005). A year of continuous measurements of three atmospheric mercury species (GEM, RGM

and Hgp) in southern Qucbec, Canada. *Atmospheric Environment*, *39*(7), 1275–1287.

Schroeder, W., & Munthe, J. (1998). Atmospheric mercury—an overview. *Atmospheric Environment*, *32*(5), 809-822.

Schuster, P. F., Krabbenhoft, D. P., Naftz, D. L., Cecil, L. D., Olson, M. L., Dewild, J. F., ... & Abbott, M. L. (2002). Atmospheric mercury deposition during the last 270 years: a glacial ice core record of natural and anthropogenic sources. Environmental science & technology, 36(11), 2303-2310.

Seigneur, C., Vijayaraghavan, K., Lohman, K., Karamchandani, P., & Scott, C. (2004). Global source attribution for mercury deposition in the United States. *Environmental Science & Technology*, *38*(2), 555–569.

Selin, N. E., & Jacob, D. J. (2008). Seasonal and spatial patterns of mercury wet deposition in the United States: North American vs. intercontinental sources. *Atmospheric Environment*, *42*, 5193–5204.

Siegel, S. M., & Siegel, B. Z. (1988). Temperature determinants of plant-soil-air mercury relationships. *Water, Air, and Soil Pollution*, *40*(3–4), 443–448.

Slemr, F., et al. "Worldwide trend of atmospheric mercury since 1995." Atmospheric Chemistry and Physics 11.10 (2011): 4779-4787.

Song, X., Cheng, I., & Lu, J. (2009). Annual atmospheric mercury species in downtown Toronto, Canada. *Journal of Environmental Monitoring : 11*(3), 660–9.

Stamenkovic, J., Lyman, S., & Gustin, M. S. (2007). Seasonal and diel variation of atmospheric mercury concentrations in the Reno (Nevada, USA) airshed. *Atmospheric Environment*, *41*(31), 6662–6672.

Surmann, P., & Zeyat, H. (2005). Voltammetric analysis using a self-renewable non-mercury electrode. *Analytical and Bioanalytical Chemistry*, *383*(6), 1009–1013.

Talbot, R., Mao, H., Scheuer, E., Dibb, J., & Avery, M. (2007). Total depletion of Hg in the upper troposphere–lower stratosphere. *Geophysical Research Letters*, *34*(23).

Weiss-Penzias, P., Jaffe, D., Swartzendruber, P., Hafner, W., Chand, D., & Prestbo, E. (2007). Quantifying Asian and biomass burning sources of mercury using the Hg/CO ratio in pollution plumes observed at the Mount Bachelor Observatory. *Atmospheric Environment*, *41*(21), 4366–4379.

Zhu, J., Wang, T., Talbot, R., Mao, H., Hall, C. B., Yang, X., … Huang, X. (2012). Characteristics of atmospheric Total Gaseous Mercury (TGM) observed in urban Nanjing, China. *Atmospheric Chemistry and Physics*, *12*(24), 12103–12118.

Vita

Name of Author: Linghui Meng

Place of Birth: Linyi, Shandong, China

Date of Birth: October 30th, 1989

Undergraduate School Attended: Bachelor of Environmental Science, 2012.

Research Experience:

Patterns of total gaseous mercury at a former brownfield in Syracuse, NY, Linghui Meng, Charles T. Driscoll, Mario Montesdeoca, Geoffrey D. Millard, Patrick McHale, Myron J Mitchell, 2016 American Geophysical Union Fall Meeting, 2016.

Influence of the remediation of a former brownfield on TGM concentrations and variation in Syracuse, NY, Linghui Meng, Syracuse University, 2016.

Wind impact on urban gaseous mercury concentration at Syracuse Center of Excellence, Linghui Meng, Charles T. Driscoll, Mario Montesdeoca, Geoffrey D. Millard, Patrick McHale, Myron J Mitchell, 2015 Syracuse Center of Excellence Annual Symposium, 2016.